Proc. Natl. Acad. Sci. USA
Vol. 88, pp. 424–428, January 1991
Biochemistry

Solution conformations of the γ-carboxyglutamic acid domain of bovine prothrombin fragment 1, residues 1–65

(molecular dynamics/crystal structure/proline isomerization)

PAUL S. CHARIFSON*, TOM DARDEN†, ALEXANDER TULINSKY§, JOSEPH L. HUGHEY*, RICHARD G. HISKEY*, AND LEE G. PEDERSEN*†¶

*Chemistry Department, University of North Carolina, Chapel Hill, NC 27599-3290; †National Institute of Environmental Health Sciences, Research Triangle Park, NC 27709; and §Department of Chemistry, Michigan State University, East Lansing, MI 48824

Communicated by Robert G. Parr, September 27, 1990 (received for review February 13, 1990)

ABSTRACT **Molecular dynamics simulations have been performed (AMBER version 3.1) on solvated residues 1–65 of bovine prothrombin fragment 1 (BF1) by using the 2.8-Å resolution crystallographic coordinates as the starting conformation for understanding calcium ion-induced conformational changes that precede experimentally observable phospholipid binding. Simulations were performed on the non-metal-bound crystal structure, the form resulting from addition of eight calcium ions to the 1–65 region of the crystal structure, the form resulting from removal of calcium ions after 107 ps and continuing the simulation, and an isolated hexapeptide loop (residues 18–23). In all cases, the 100-ps time scale seemed adequate to sample an ensemble of solution conformers within a particular region of conformation space. The non-metal-containing BF1 did not unfold appreciably during a 106-ps simulation starting from the crystallographic geometry. The calcium ion-containing structure (Ca-BF1) underwent an interesting conformational reorganization during its evolution from the crystal structure: during the time course of a 107-ps simulation, Ca-BF1 experienced a trans → cis isomerization of the γ-carboxyglutamic acid-21 (Gla-21)—Pro-22 peptide bond. Removal of the calcium ions from this structure followed by 114 ps of additional molecular dynamics showed significant unfolding relative to the final 20-ps average structure of the 107-ps simulation; however, the Gla-21—Pro-22 peptide bond remained cis. A 265-ps simulation on the termini-protected hexapeptide loop (Cys-18 to Cys-23) containing two calcium ions also did not undergo a trans → cis isomerization. It is believed that the necessary activation energy for the transitional event observed in the Ca-BF1 simulation was largely supplied by global conformational events with a possible assist from relief of intermolecular crystal packing forces. The presence of a Gla preceding Pro-22, the inclusion of Pro-22 in a highly strained loop structure, and the formation of two long-lived salt bridges prior to isomerization may all contribute to this finding.**

Prothrombin, a protein of central importance in the coagulation cascade, is converted to thrombin by the action of a macromolecular complex involving the protease factor Xa bound to the membrane protein factor Va. The conversion occurs on the surface of the membrane; binding of the substrate, prothrombin, is mediated by calcium ions. Magnesium ions do not support the prothrombin–membrane interaction (1–6). Bovine fragment 1 (BF1) corresponds to the amino-terminal 156 residues of bovine prothrombin; the first 33 amino acids contain 10 γ-carboxyglutamic acid (Gla) residues. These Gla residues are created by means of post-translational modification of glutamic acid residues in the presence of a vitamin K-dependent carboxylase and endow prothrombin with its essential calcium-mediated phospholipid-binding properties (1). The Gla domain of prothrombin has classically referred to the first 48 residues of the amino-terminal region and is highly conserved in other protein members of the coagulation cascade: factors VII, IX, and X of the procoagulant cascade and proteins C, S, and Z of the anticoagulant loop. Even though they are highly homologous (65–70%) in the Gla domain, these proteins display different metal-binding properties, as the number of Gla residues ranges from 9 to 12 (7). An important question presents itself here as to whether the structural differences are relevant to corresponding differences in function. With the aid of the calcium-containing BF1 (Ca-BF1) crystal structure (7), we can approximate the other Gla-containing proteins and perform simulations to determine differences in the presence and absence of divalent ions.

Although there is a large body of experimental observations pertaining to Ca-BF1, there was little structural information known (8–12) until the recent crystallographic determination. In the absence of calcium ions, the first 35 residues of the Gla domain are disordered in the apo structure (9, 10). Thus, calcium-mediated phospholipid binding might initially depend on a calcium ion-induced folding transition of the amino-terminal 35 residues (7). An interesting experimental observation by Nelsestuen (1) showed a biphasic fluorescence quenching behavior for BF1 upon the addition of metal ions. This quench of intrinsic tryptophan fluorescence parallels the phospholipid-binding behavior of BF1 and bovine prothrombin. An initial rapid quench (<1 s) is followed by a slow quenching phase (>10 min); the latter has been hypothesized by Marsh *et al.* (13) to represent an isomerization of the Gla-21—Pro-22 peptide bond from trans to cis. The initial fluorescence quenching event may be the result of an interaction of the disulfide of the small conserved hexapeptide loop (residues 18–23) with a three-dimensional cluster of aromatic residues (Phe-41, Trp-42, and Tyr-45), which is also highly conserved (7). The proline isomerization hypothesis is consistent with both experimental (14–21) and theoretical (22) investigations, which indicate that proline isomerization may be the rate-limiting step in protein folding pathways.

Since the isomeric structure of Pro-22 is not clear at the present level of refinement of the crystallographic structure (2.8-Å resolution) and the same applies to the location of calcium ion positions (7), we have used molecular dynamics (MD) to generate potential solution conformations by allowing relaxation of the crystallographic structure of Ca-BF1 under several conditions. Analysis of these simulations is then performed in light of the previous observations.

The publication costs of this article were defrayed in part by page charge payment. This article must therefore be hereby marked "*advertisement*" in accordance with 18 U.S.C. §1734 solely to indicate this fact.

Abbreviations: BF1, bovine fragment 1; MD, molecular dynamics; rms, root-mean-square; Gla, γ-carboxyglutamic acid; Ca-BF1, calcium-containing BF1.

¶To whom reprint requests should be addressed at *.

COMPUTATIONAL METHODS

General. The first 65 residues [Ca-BF1-(1–65)] were chosen as a model of BF1 because recent evidence shows this region to functionally constitute the Gla domain (7, 23). An N-methyl cap was graphically placed on Asn-65 for all Gla domain calculations by using the MULTI software (24). All calculations were performed using AMBER version 3.1 (25) under the following conditions unless otherwise noted: hydrogens were added to the heavy atom crystallographic coordinates followed by immersion in a periodic box containing TIP3P waters. Gla parameters came from ref. 26. For the metal-containing calculations, the non-bond parameters employed were r_ε = 1.65 Å, ε = 0.1 kcal/mol for calcium; r_ε = 1.10 Å, ε = 0.1 kcal/mol for magnesium (27). Structures were initially minimized (100 cycles of steepest descent followed by conjugate gradient minimization) to a root-mean-square (rms) gradient of 0.1 kcal·mol^{-1}·Å^{-1} by employing an 8.0-Å residue-based non-bond cutoff, constant dielectric function, all-atom force field, and constant pressure with periodic boundary conditions. MD simulations were then performed employing velocity scaling to maintain a constant temperature of 300 K. A 1.0-fs time step was used and the SHAKE (25) algorithm was applied to constrain all bonds involving hydrogens. A mass of 3 atomic mass units was used for all hydrogens, and the non-bond list was updated every 50 steps.

All calculations were performed on a Cray-YMP/8-432 supercomputer at the North Carolina Supercomputer Center. Molecular dynamics trajectories were analyzed statistically (24, 25) as well as graphically by means of a movie (24) of the simulation on a Silicon Graphics IRIS 240 GTX workstation.

Simulation of Ca-BF1-(1–65). Although the crystal structure was solved in the presence of calcium ions, the actual calcium ion positions are not known at 2.8-Å resolution. Potential calcium positions were estimated by energy minimization of the crystal structure using a distance-dependent dielectric function and an 8.0-Å non-bond cutoff. One hundred cycles of steepest descent minimization were initially performed followed by 2100 cycles of conjugate gradient minimization. rms comparisons using the COMPARE program (28) were then performed on all Gla oxygen positions. It was rationalized that any previously metal-bound ligands (i.e., oxygen atoms) would have moved significantly from the crystallographic positions. Analysis of oxygen positions with an rms deviation of >2.0 Å from the crystal structure showed 8 of the 10 Gla residues to be likely calcium site candidates. This prediction is in reasonable agreement with Scatchard analysis based on equilibrium dialysis studies, which report either six (5, 29) or seven (30) significant calcium binding sites in BF1. One of these sites may lie outside of the 1–65 sequence examined in the present study (A.T., unpublished data; ref. 31). Calcium ions were graphically placed in the eight rms-predicted metal-binding sites of the original crystallographic structure in an attempt to maximize potential Gla–metal interactions while avoiding steric conflicts or disruption of any stabilizing (e.g., salt bridge) interactions. The system was then subjected to the general methods described above, and molecular dynamics was performed for 107 ps.

Another simulation included removal of the metal ions after 107 ps, resolvation of the non-metal-bound protein, and reminimization in a water bath followed by 114 ps of MD, as previously described for the calcium structure.

Simulation of Non-Metal-Containing BF1 (Residues 1–65). The original crystal coordinates (N-methyl-capped residues 1–65) were minimized initially *in vacuo*, then solvated in a water bath, reminimized, and subjected to 106 ps of MD simulation according to the methodology described above.

Simulation of the Isolated Hexapeptide Loop (Residues 18–23). Residues 18–23 were removed from the original crystal structure, and the amino terminus (Cys-18) was capped with an acetyl group while the carboxyl terminal (Cys-23) was protected with an N-methyl group. Two calcium ions were graphically placed between Gla residues 20 and 21, and this system was minimized in a water bath and subjected to 265 ps of MD according to the usual procedure.

RESULTS AND DISCUSSION

The prediction of potential macromolecule solution conformations can be facilitated by the use of MD simulations. If the starting geometry is derived from a crystal structure, it is not surprising that time evolution in a thermal water bath may, in some cases, allow for significant structural changes from the initial conformation influenced by crystal packing forces. Differences between crystal structures and solution structures of proteins as determined by two-dimensional NMR are known (32). Although MD can be used to generate potential solution structures, a difficulty is that it is not always clear how long a given MD simulation should be performed with respect to the time scale of observable conformational events to conclude a reasonable solution structure has been attained.

Simulation of Ca-BF1-(1–65). We performed 107 ps of MD on Ca-BF1-(1–65); an analysis of the extent of atomic displacement of backbone (C^α—C—N) atoms from the crystallographic geometry with respect to time for this simulation is presented in Fig. 1. It appears that after some substantial reorganization of structure (over the first 45 ps), the overall rms deviation of backbone atoms for the remainder of the trajectory is <1 Å. This is indicative of an equilibrated solution structure within the region of conformational space that was explored by this calculation. Having found an adequate sampling time, evaluation of overall motion on a residue basis was performed. An average structure was calculated for the final 20 ps of the simulation and compared to the crystal structure in terms of α-carbon rms deviations (Fig. 2). The region of Ca-BF1-(1–65) experiencing the greatest amount of motion over the course of the simulation was in the amino-terminal end of the protein from Ala-1 to Phe-5. In the crystal structure, Ala-1 appears to be hydrogen bonded to the backbone carbonyls of Leu-19 and Gla-20; in solution, however, the amino hydrogens of Ala-1 are probably exchanging with solvent, thereby no longer restricting the amino terminus in this manner. A large change in the envi-

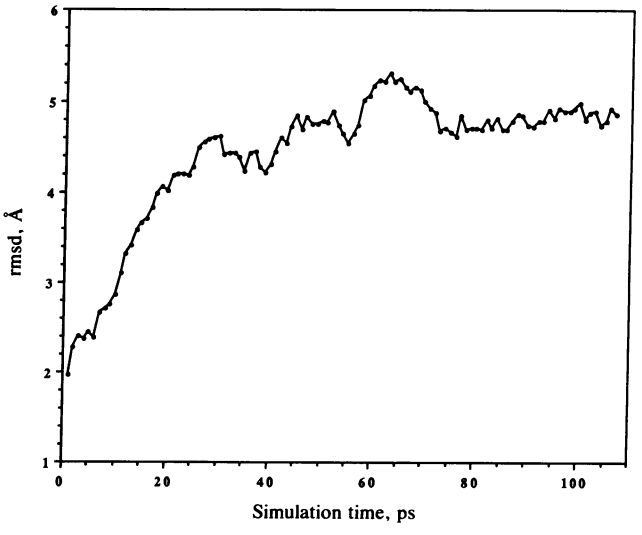

FIG. 1. rms deviation (rmsd) of backbone atoms of Ca-BF1-(1–65) from crystal structure versus simulation time.

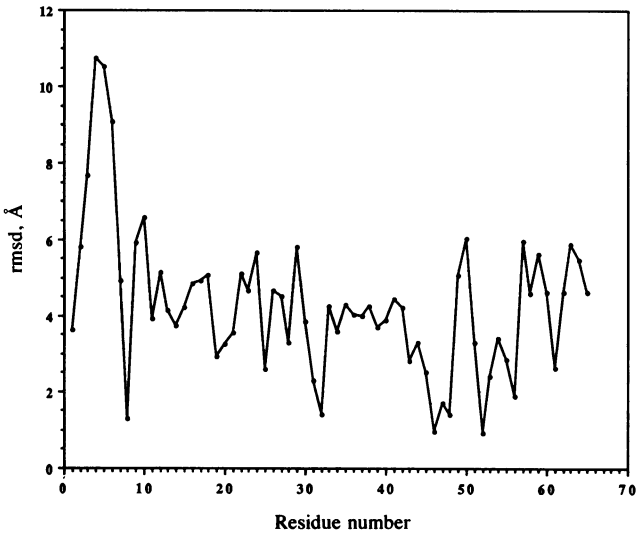

FIG. 2. rms deviation (rmsd) of α-carbons of Ca-BF1-(1–65) for the final 20-ps average structure (total time of simulation = 107 ps) versus crystal structure. The comparison was residue based.

ronment around Arg-10 is also seen in Fig. 2. In the crystal structure, Arg-10 does not interact with other Gla domain residues; however, upon MD, strong hydrogen bonds form with the backbone carbonyl oxygen of Val-9 and one of the carboxylate oxygens of Gla-7, which then seem to persist through the course of the simulation. The other regions of significant deviation include portions of the two disulfide loops of the Gla domain residues (18–23 and 48–61). These loops appear to be stacked in the crystal structure and were modeled to initially interact by means of a single calcium ion bridging residues 20 and 52–54.

Calcium Coordination. Evaluation of the eight calcium sites for an indication of cooperative motion over the course of the simulation was also considered. It has been proposed that there are from one to three tight-binding calcium sites in Ca-BF1, but only one of these sites may be necessary for inducing the conformational changes required of phospholipid binding (30). It was, therefore, of interest to analyze the coordination environment of each calcium before (0 ps) and after (107 ps) the simulation to determine if such tight sites could be identified. Reasonable criteria for a tight-binding calcium site might be (*i*) involvement of more than one Gla residue and (*ii*) at least three short O-Ca^{2+} distances ($r_{Ca\text{-}O} \leq$ 2.6 Å). With these criteria, we find, at 0 ps, two sites with three Gla O-Ca^{2+} coordinations {[Gla-7, Gla-26 (2)] and [Gla-17, Gla-27 (2)]}. At 107 ps we find five sites: one of these sites contains four Gla O-Ca^{2+} coordinations {[Gla-7 (2), Gla-26 (2)], two [Gla-20 (2), Gla-21], [Gla-17, Gla 27 (2)], and [Gla 15 (2), Gla 30]}. The Gla-7, Gla-26 site is especially of interest; if Gla-7, -8, and -33 are modified to γ-methyleneglutamyl residues by means of a Tb^{3+}/formaldehyde-morpholine procedure (33), the modified protein loses most of the ability to bind phospholipid, and Ca^{2+} binding is weaker and no longer cooperative. Further analysis shows that, at the beginning of MD, there is a calcium ion bridging Gla-20 of the hexapeptide disulfide loop (Cys-18 to Cys-23) and the backbone carboxyl oxygens of Arg-52, Asn-53, and Pro-54 of the tetradecapeptide loop (Cys-48 to Cys-61). Graphical display of the simulation shows that Gla-20 "pulls" this calcium away from the tetradecapeptide loop and then begins to share this calcium with Gla-21 along with a second calcium ion, which was weakly bound to Gla-20 at 0 ps. By the end of the simulation, Gla residues 20 and 21 are involved in a stable two-Gla, two-Ca^{2+} ion site, which has persisted for over 50 ps.

Isomerization of the Gla-21—Pro-22 Peptide Bond. A significant result to arise from this work was the transitional conformation change surrounding the Gla-21—Pro-22 peptide bond. The crystal structure of Ca-BF1, which cannot presently distinguish between cis and trans isomer, has this peptide to be in the trans conformation; however, during the 107-ps MD simulation, this bond isomerized to the cis conformer while all other peptide bonds in the structure remained trans. This transition is illustrated in Fig. 3 by monitoring the absolute torsional deviation of the Gla-21—Pro-22 peptide from 180° as a function of time. It is apparent that, for the first 83 ps of the simulation, the trans isomer is favored, but, at this transition time, the barrier to isomerization is overcome. Although the $\Delta G^{\ddagger}$ for trans → cis isomerism for most linear peptides is 20 ± 1 kcal/mol (34), $\Delta G^{\ddagger}$ for proline isomerization in small cyclic peptides is more on the order of 15 ± 1 kcal/mol as determined by ^{13}C and ^{1}H NMR in aqueous solution (35). An analysis of the potential energies of the metal-bound protein at the MD conformations over the isomerization period (82–85 ps) is given in Fig. 3 *Inset* to illustrate the barrier present in this system. A five-point average of the data predicts an energy barrier of ≈9 kcal/mol; the cis structure is more stable by about 17 kcal/mol. It has been proposed that in cyclic peptides the rates of proline isomerization are 6-fold higher (19) than corresponding linear peptides. It has also been shown that the steric contribution of the residue preceding proline has an effect on the activation barrier for isomerization (18, 36). The presence of Gla-21 preceding Pro-22 might contribute to a lowering of the activation barrier since it is not a commonly encountered residue. It is unlikely, however, that cis → trans isomerizations are localized events: the transitions between energy minima probably involve concerted motion of many different portions of the molecule. In fact, when the isolated hexapeptide (Cys-18 to Cys-23) with two calcium ions (between Gla residues 20 and 21) was subjected to 265 ps of MD (identical conditions to the full 1–65 region simulation), proline isomerization did not occur. Further evidence for a concerted isomerization mechanism is evident from the dynamics of internal salt bridge formation during the simulation. At the beginning of the simulation (0 ps), Arg-16 is salt bridged to Asp-39; immediately prior to the transition, at 75 ps, while the Gla-21—Pro-22 peptide is still trans, two long-lived sets of salt bridges have formed between Arg-16

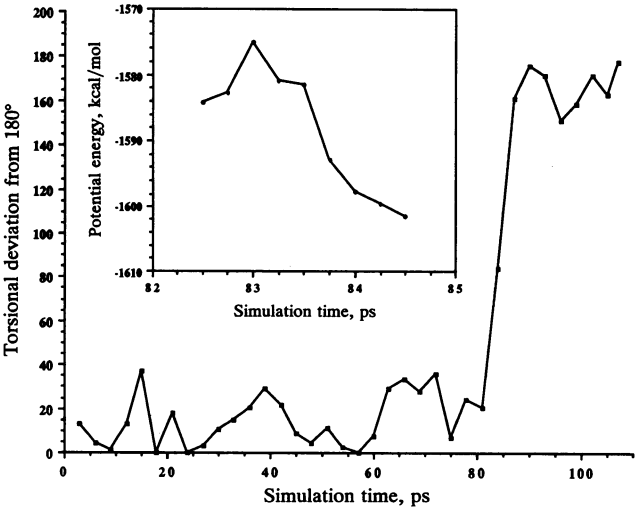

FIG. 3. Deviation (absolute) of torsional angle, ω, for Gla-21—Pro-22 as a function of simulation time. (*Inset*) MD single-point potential energies expressed as a five point average versus simulation time. Only the protein atoms were used to calculate the potential energy; the potential energy was evaluated every 0.25 ps.

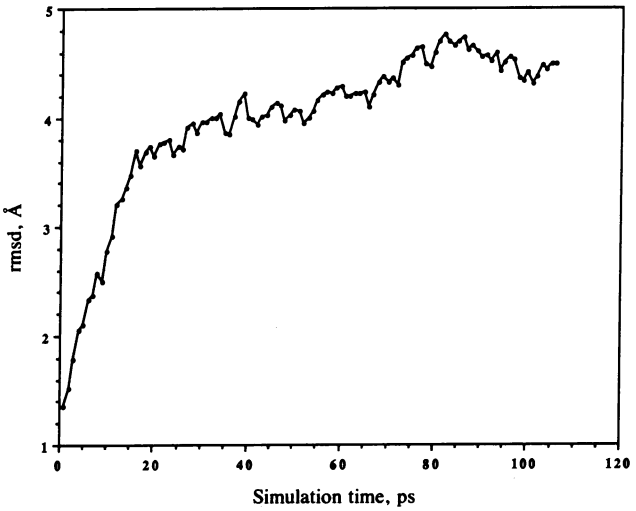

FIG. 4. rms deviation of backbone atoms of non-metal-bound BF1-(1–65) from crystal structure versus simulation time.

and Glu-49 and between Gla-20 and Arg-55. The isomerization then occurs, and the integrity of these salt bridges is maintained for the remainder of the simulation. One possible rationalization for the proline isomerization is that (*i*) refolding, combined with (*ii*) the potential lowering of the activation barrier by Pro-22 being contained within a loop structure or (*iii*) the presence of an adjacent Gla, as well as (*iv*) the stabilizing salt bridges and the "jump" of the calcium ion from the tetradecapeptide loop to Gla-20, all appear to contribute to the isomerization to produce a more stable solution conformation. An analysis of intermolecular packing between symmetry-related molecules (24) in the crystal structure of Ca-BF1 shows significant interactions between Gla domains that could be related to the large degree of structural reorganization that has occurred during the simulation. Distances ranging from 3 to 5 Å between side-chain oxygens of Gla-7 of one molecule of Ca-BF1-(1–65) and Glu-63 of an adjacent molecule could be due to calcium bridging in the crystal structure. A pair of salt bridges between Gla-8 and Arg-55 and between Arg-10 and Gla-33 of neighboring structures also appears to be significant while Gla-21 and Asn-13 of adjacent molecules share a hydrogen bond.

Removal of Calcium Ions from the 107-ps MD Structure. The eight calcium ions were removed from the 107-ps MD Ca-BF1-(1–65) structure with cis proline at position 22. Upon resolvation and further MD for 114 ps, considerable reorganization occurred. The rms deviation of all backbone atoms relative to the backbone atom positions of the average structure for the final 20 ps of the initial simulation (i.e., 87–107 ps) was compared to the 114-ps simulation. It is noteworthy that the overall deviation is quite large (>3.0 Å), indicating that the calcium ions were intimately involved in the maintenance of tertiary structure. It is also of note that Pro-22 remains in the cis conformation, although other regions of the protein appear to be changing dramatically. Bajorath *et al.* (37) recently observed some significant crystallographic structural changes in the subtilisin-type enzyme proteinase K upon the removal of calcium ions, which translated to a decrease in enzymatic activity.

Molecular Dynamics of the BF1 Crystal Structure Without Calcium. In a control simulation, BF1-(1–65) was subjected to 106 ps of MD with no calcium ions present. In contrast to the Ca-BF1 simulation, no trans → cis isomerization of Pro-22 was observed. A comparison of backbone atom rms deviation for the 106-ps simulation with the crystal structure is shown in Fig. 4. The 100-ps time scale seemed adequate for sampling conformation space based upon the final 30 ps of the simulation (Fig. 4). Although the equilibrated portions of both the metal-bound and non-metal-bound simulations (Figs. 1 and 4, respectively) appear to be similar in overall magnitude of deviation from the crystal structure, the portions of the protein that have moved are quite different (the rms difference between backbone atoms in the average Ca-BF1 structure and the average non-metal BF1 structure is 4.7 Å). A least-squares fit between the α-helical portions (residues 35–47) of the crystal structure (Fig. 5*A*, thick lines) and average (final 20 ps) Ca-BF1-(1–65) structure (Fig. 5*A*, thin lines) was performed since the α-helical portion of the protein exhibits the least amount of overall motion in all simulations. The same least-squares comparison was performed on the crystal structure and the average (final 20 ps) structure of the non-metal-bound simulation [Fig. 5*B*: thick lines, crystal structure; thin lines, average structure (86–106 ps)]. From these comparisons, it becomes clear that the average calcium structure has its 1–34 domain in a different orientation with respect to the crystal structure than does the average non-metal-bound structure even though the rms deviations for both helical regions from the crystal structure are similar

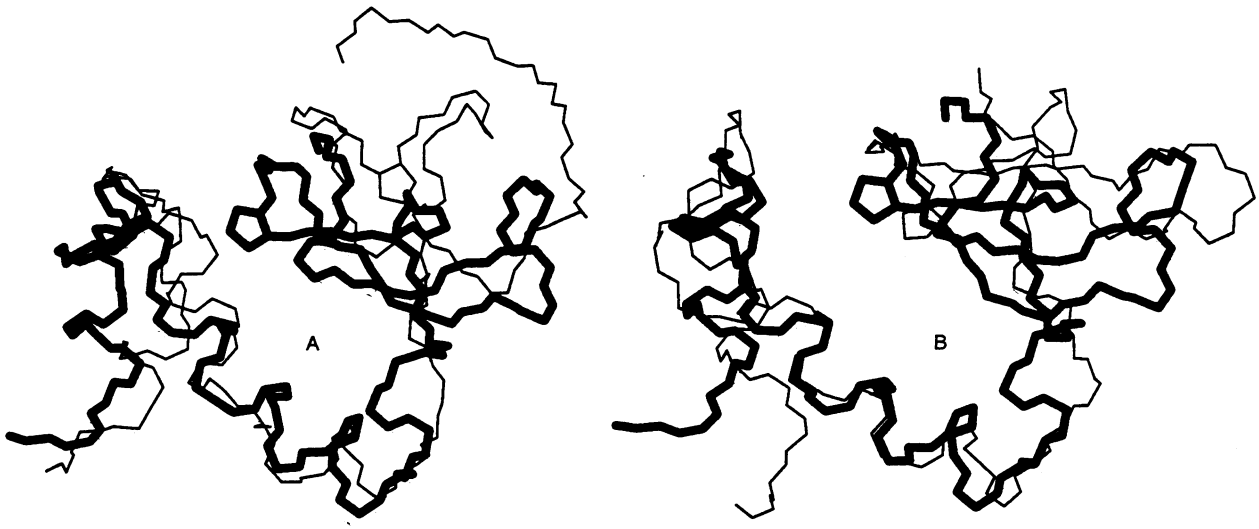

FIG. 5. (*A*) View of least-squares fit of crystal structure (thick lines) and average Ca-BF1-(1–65) structure (final 20 ps, thin lines). (*B*) View of least-squares fit of crystal structure (thick lines) and average non-metal-bound BF1-(1–65) structure (final 20 ps, thin lines). In both cases the least-squares fit was performed on α-helical residues 35–47.

(calcium structure, 1.5 Å; non-calcium structure, 1.2 Å). This might be due to the fact that the Gla-containing region of the calcium-bound structure can attain a solution conformation that is inaccessible to the non-metal-bound structure. The lack of unfolding during this simulation was unexpected, especially since significant unfolding was observed when calcium ions were removed from the 107-ps Ca-BF1 simulation structure. When the Gla-21—Pro-22 peptide bond is trans, the protein might be in one favorable energy minimum, which remains stable even in the absence of calcium, but which does not bind phospholipid. However, when isomerization to the cis peptide occurs, new conformations are attainable that require calcium for maintenance of tertiary structure, which might be required of phospholipid binding.

CONCLUSIONS

The computational methodologies presented illustrate the usefulness of MD in uncovering possible solution conformations starting with a crystal structure. The Ca-BF1 simulation, for instance, provides us with a possible calcium-induced phospholipid-binding conformation.

During the various simulations, several unexpected results were obtained: the calcium ion-containing structure (Ca-BF1) underwent a trans → cis isomerization about the Gla-21—Pro-22 peptide bond, the only peptide bond to do so, whereas the non-metal-containing BF1 structure did not, and no significant unfolding occurred. Removal of the calcium ions from the structure followed by additional MD showed significant unfolding relative to the final 20-ps average calcium structure; however, the Gla-21—Pro-22 peptide remained cis. A lengthy simulation on the isolated hexapeptide loop (Cys-18 to Cys-23) containing two calcium ions also did not undergo a trans → cis isomerization. The necessary activation energy for the transitional event observed in the Ca-BF1 simulation was probably largely dependent upon global conformational events and by relief of intermolecular crystal packing forces as evidenced by the lack of trans → cis isomerization in the isolated hexapeptide loop simulation. Clearly, the chances of having observed a trans → cis isomerization on so short a time scale (100 ps), even with a lowered activation energy (≈9 kcal/mol), are unlikely without other considerations. The presence of a Gla preceding Pro-22, the inclusion of Pro-22 in a highly strained loop structure, the jump of Ca^{2+} from the tetradecapeptide loop to the hexapeptide loop, and the formation of two long-lived salt bridges prior to isomerization may all contribute to the isomerization. These may be the critical conformational events that lead to the phospholipid-binding conformation in the calcium-bound species and that is unattainable in the non-metal-bound species. Ongoing simulations for which the calcium ions have been replaced with magnesium ions (simulation length = 113 ps) also exhibit the trans → cis isomerization of the Gla-21—Pro-22 peptide bond (81–83 ps); however, preliminary results suggest significant structural differences from the average Ca-BF1 structure consistent with the inability of magnesium to mediate phospholipid binding (1–6). For example, the difference between backbone deviations for the average final 20-ps Ca-BF1 and Mg-BF1 structures is 3.9 Å.

Although our initial assignment of calcium positions was largely qualitative, the coordination analysis is suggestive. Our results support current hypotheses (7, 23), which expand the functional definition of the Gla domain to include residues 1–65. We further conclude that one tight-binding calcium site lies between Gla residues 7 and 26, whereas another consists of an unusual two-metal, two-Gla site between Gla residues 20 and 21.

The authors acknowledge support of the National Institutes of Health through Grants HL-27995 (L.G.P.), HL-20161 (R.G.H.), HL-23609 (R.G.H. and L.G.P.), and HL-25942 (A.T.). We thank Professor J. Phillip Bowen for access to his molecular modeling laboratory at the University of North Carolina and the North Carolina Supercomputer Center for access to their Cray YMP/8-432. We also thank Howard Smith and Pam Johnson for their programming assistance. We especially acknowledge P. Kollman and U. C. Singh for consistently providing source codes for their dynamics programs.

1. Nelsestuen, G. L. (1976) *J. Biol. Chem.* **251,** 5648–5656.
2. Suttie, J. W. & Jackson, C. M. (1977) *Physiol. Rev.* **57,** 1–70.
3. Nelsestuen, G. L., Zytkovicz, T. H. & Howard, J. B. (1974) *J. Biol. Chem.* **249,** 6347–6350.
4. Stenflo, J., Fernlund, P., Egan, W. & Roepstorff, P. (1974) *Proc. Natl. Acad. Sci. USA* **71,** 2730–2733.
5. Bajaj, S. P., Butkowski, R. J. & Mann, K. G. (1976) *J. Biol. Chem.* **250,** 2150–2156.
6. Nesheim, M. E., Hibbard, L. S., Tracy, P. B., Bloom, J. W., Myrmel, K. H. & Mann, K. G. (1980) in *The Regulation of Coagulation,* eds. Mann, K. G. & Taylor, F. B. (Elsevier, New York), pp. 145–160.
7. Soriano-Garcia, M., Park, C. H., Tulinsky, A., Ravichandran, K. G. & Skrzypczak-Jankun, E. (1989) *Biochemistry* **28,** 6805–6810.
8. Olsson, G., Andersen, L., Lindquist, O., Sjolin, L., Magnusson, S., Peterson, T. E. & Sottrup-Jensen, L. (1982) *FEBS Lett.* **145,** 317–322.
9. Park, C. H. & Tulinsky, A. (1986) *Biochemistry* **25,** 3977–3982.
10. Tulinsky, A., Park, C. H. & Skrzypczak-Jankun, E. (1988) *J. Mol. Biol.* **202,** 885–901.
11. Harlos, K., Holland, S. K., Boys, C. W. G., Burgess, A. I., Esnouf, M. P. & Blake, C. C. F. (1987) *Nature (London)* **330,** 82–84.
12. Harlos, K., Boys, C. W. G., Holland, S. K., Esnouf, M. P. & Blake, C. C. F. (1987) *FEBS Lett.* **224,** 97–103.
13. Marsh, H. C., Scott, M. E., Hiskey, R. G. & Koehler, K. A. (1979) *Biochem. J.* **183,** 513–517.
14. Brandts, J. F., Halvorson, H. R. & Brennan, M. (1975) *Biochemistry* **14,** 4953–4963.
15. Grathwohl, C. & Wuthrich, K. (1979) *Biopolymers* **15,** 2025–2041.
16. Lin, L. & Brandts, J. F. (1978) *Biochemistry* **17,** 4102–4110.
17. Bachinger, H. P., Bruckner, P., Timpl, R. & Engel, J. (1978) *Eur. J. Biochem.* **90,** 605–613.
18. Cook, K. H., Schmid, F. X. & Baldwin, R. L. (1979) *Proc. Natl. Acad. Sci. USA* **76,** 6157–6161.
19. Grathwohl, C. & Wuthrich, K. (1981) *Biopolymers* **20,** 2623–2633.
20. Lin, L. N. & Brandts, J. F. (1983) *Biochemistry* **22,** 559–563.
21. Nall, B. T. (1985) *Comments Mol. Cell. Biophys.* **3,** 123–143.
22. Levitt, M. (1981) *J. Mol. Biol.* **145,** 251–263.
23. Schwalbe, R. A., Ryan, J., Stern, D. M., Kisiel, W., Dahlback, B. & Nelsestuen, G. L. (1989) *J. Biol. Chem.* **264,** 20288–20296.
24. Darden, T., Johnson, P. & Smith, H. (1989) MULTI (Natl. Inst. Environ. Health Sci., Research Triangle Park, NC), Version 1.1.
25. Singh, U. C., Weiner, P. K. & Kollman, P. A. (1988) AMBER, A Molecular Mechanics and Dynamics Program (Univ. of California, San Francisco), Version 3.1.
26. Maynard, A. T., Eastman, E. A., Darden, T., Deerfield, D. W., Hiskey, R. G. & Pedersen, L. G. (1988) *Int. J. Pept. Protein Res.* **31,** 137–149.
27. Cabaniss, S. E., Pugh, K. C., Charifson, P. S., Pedersen, L. G. & Hiskey, R. G. (1990) *Int. J. Pept. Protein Res.* **36,** 79–85.
28. Deerfield, D. W. & York, D. (1989) COMPARE program, Pittsburgh Supercomputing Center, Version 1.1.
29. Pendergast, F. G. & Mann, K. G. (1977) *J. Biol. Chem.* **252,** 840–850.
30. Deerfield, D. W., Berkowitz, P., Olson, D. L., Wells, S., Hoke, R. A., Koehler, K. A., Pedersen, L. G. & Hiskey, R. G. (1986) *J. Biol. Chem.* **261,** 4833–4839.
31. Welsch, D. J. & Nelsestuen, G. L. (1988) *Biochemistry* **27,** 4946–4952.
32. Bax, A. (1989) *Annu. Rev. Biochem.* **58,** 223–256.
33. Zapata, G. A., Berkowitz, P., Noyes, C. M., Pollock, J. S., Deerfield, D. W., III, Pedersen, L. G. & Hiskey, R. G. (1988) *J. Biol. Chem.* **263,** 8150–8156.
34. Stewart, W. E. & Siddall, T. H., III (1970) *Chem. Rev.* **70,** 517–551.
35. Deber, C. M., Fossel, E. T. & Blout, E. R. (1974) *J. Am. Chem. Soc.* **96,** 4015–4017.
36. Kopple, K. D., Zhu, P. P. & Go, A. (1983) *Biopolymers* **22,** 153–156.
37. Bajorath, J., Raghunathan, S., Hinrichs, W. & Saenger, W. (1989) *Nature (London)* **337,** 481–484.